

# STUDIES ON LUMINOUS REGION, PILE-UP AND PERFORMANCE FOR HL-LHC SCENARIOS\*

L. Medina<sup>1†</sup>, Universidad de Guanajuato, León, Mexico  
 G. Arduini, R. Tomás, CERN, Geneva, Switzerland  
<sup>1</sup>also at CERN, Geneva, Switzerland

## Abstract

Studies on luminous region and pile-up density are of great interest for the experiments at the future High Luminosity LHC (HL-LHC) in order to optimize the detector performance. The evolution of these parameters at the two main interaction points of the HL-LHC along optimum physics fills is studied for the baseline and alternative operational scenarios with the latest set of parameters, including a refined description of the longitudinal bunch profile. Results are discussed in terms of a new figure-of-merit, the effective pile-up density.

## INTRODUCTION

Since its original design [1], several parameters of interest of the High Luminosity LHC (HL-LHC) have changed; for example the number of crab cavities has been halved [2], and the RMS Gaussian bunch length has been increased to  $\sigma = 9$  cm (or  $4\sigma = 1.2$  ns), to ensure stability [3].

Five scenarios are presented in this work, namely the baseline, 8b+4e, 200 MHz, and Flat –that make use of two crab cavities (CCs) for the compensation of the crossing angle–, and a fifth case without CCs. Round and/or flat optics are used at the two main interaction points (IPs), and their parameters are listed in Table 1; in the case of round optics, the CCs provide only partial compensation (380  $\mu$ rad). The long-range beam-beam separation is  $12.5\sigma$  for all scenarios –an optimistic assumption for the case without CCs that has yet to be demonstrated. The yearly integrated performance, defined as in [1], assumes 160 days with 50% and 58% efficiency for the nominal and ultimate operation, respectively; complete simulations parameters are described in [4]. Dynamic aperture studies for a wide range of settings are presented in [5].

In the first section we describe the q-Gaussian distribution used to characterize the longitudinal bunch profile [6, 7]. A new parameter, the effective pile-up density, is introduced afterwards as a figure-of-merit to evaluate the different operational alternatives in terms of detector performance [8, 9]. The results on integrated luminosity, pile-up and luminous region are then presented and discussed for the baseline and alternative scenarios.

## q-GAUSSIAN BUNCH PROFILE

Simulations are performed with a bunch profile described by a Tsallis q-Gaussian distribution [10] centred around

\* Research supported by the HL-LHC project and the Beam project (CONACYT, Mexico).

† lmedinam@cern.ch

the origin, with deformation parameter  $q = 3/5$ , and scale parameter  $\beta = 10/S^2$ , i.e.

$$\lambda(s) = \frac{32}{5\pi S} \left(1 - \frac{4s^2}{S^2}\right)^{5/2}, \quad -\frac{S}{2} \leq s \leq \frac{S}{2}, \quad (1)$$

with RMS value

$$\sigma_\lambda = \frac{S}{4\sqrt{2}}, \quad (2)$$

in contrast with previous simulations that consider Gaussian densities [11]. This is the case in the LHC and it is justified for the HL-LHC; such a description is valid at the beginning of the fill, the bunch profile tends to Gaussian at the end of it (due to synchrotron radiation damping), and then back to q-Gaussian after bunch flattening.

Bunch length is usually described by its Gaussian RMS value. In operation, however, the full width at half maximum (FWHM) of the longitudinal distribution is used instead since stability threshold is related to it. In particular for Eq. (1),

$$\text{FWHM}(\lambda) = S \sqrt{1 - 2^{-2/5}}. \quad (3)$$

For the q-Gaussian distribution to have the same FWHM than a Gaussian distribution, the relation between their RMS values is

$$\sigma_\lambda = \frac{\sigma}{2} \sqrt{\frac{\ln 2}{1 - 2^{-2/5}}} \approx 0.846\sigma. \quad (4)$$

For the latest Gaussian RMS value of  $\sigma = 9$  cm, this implies  $\sigma_\lambda = 7.6$  cm and  $\text{FWHM} = 21.2$  cm for the q-Gaussian description of the bunch profile. The bunch length (Table 1) is kept constant along the simulations of the fill in all scenarios, except for the 200 MHz alternative, where it decreases due to cooling. The Gaussian bunch length is also longer (15 cm) in this scenario, which corresponds to  $\sigma_\lambda = 12.7$  cm and a FWHM of 35.5 cm. Furthermore, the longitudinal stability is guaranteed by the existence of 400 MHz cavities,

Table 1: Beta Function, Emittance and Crossing Angle for the HL-LHC Baseline and Alternative Scenarios

| Parameter            | Unit            | Baseline | 8b+4e | 200 MHz | Flat | No CC |
|----------------------|-----------------|----------|-------|---------|------|-------|
| $\beta_x^*$          | cm              | 20       | 20    | 40      | 40   | 40    |
| $\beta_y^*$          | cm              | 20       | 20    | 15      | 15   | 15    |
| Norm. emittance      | $\mu\text{m}$   | 2.5      | 2.2   | 2.5     | 2.5  | 2.5   |
| Total crossing angle | $\mu\text{rad}$ | 510      | 480   | 360     | 360  | 360   |
| RMS bunch length     | cm              | 7.6      | 7.6   | 12.7    | 7.6  | 7.6   |
| FWHM                 | cm              | 21.2     | 21.2  | 35.3    | 21.2 | 21.2  |

Table 2: Luminosity, Pile-up, Levelling Time, and Fill Duration for the HL-LHC Baseline and Alternative Scenarios

| Parameter                     | Unit                                     | Nominal  |       |         |      |       | Ultimate |       |         |      |       |
|-------------------------------|--|----------|-------|---------|------|-------|----------|-------|---------|------|-------|
|                               |  | Baseline | 8b+4e | 200 MHz | Flat | No CC | Baseline | 8b+4e | 200 MHz | Flat | No CC |
| Levelled luminosity           | $10^{34} \text{ cm}^{-2} \text{ s}^{-1}$ | 5.0      | 3.8   | 5.0     | 5.0  | 5.0   | 7.5      | 5.4   | 7.5     | 7.5  | 7.5   |
| Pile-up                       | 1  | 132      | 140   | 132     | 132  | 132   | 197      | 200   | 197     | 197  | 197   |
| Levelling time                | h  | 5.8      | 5.8   | 5.2     | 5.8  | 4.8   | 2.5      | 3.0   | 1.8     | 2.5  | 0.9   |
| Fill duration                 | h  | 7.8      | 7.6   | 7.7     | 7.8  | 7.2   | 5.3      | 5.3   | 5.4     | 5.3  | 5.3   |
| Integrated luminosity         | $\text{fb}^{-1}/160 \text{ days}$        | 234      | 177   | 229     | 234  | 211   | 321      | 242   | 305     | 322  | 274   |
| Diff. w.r.t. nominal baseline | –  | –        | –24%  | –2%     | 0%   | –10%  | +38%     | +4%   | +31%    | +38% | +17%  |

which in turn, can be used for double RF harmonic operation. In the latter case, the total voltages per beam in each system are  $V_{200\text{MHz}} = 6 \text{ MV}$  and  $V_{400\text{MHz}} = 3 \text{ MV}$  for both bunch-shortening or bunch-bunch-lengthening modes [12]; no additional space space is needed for the 200 MHz scenario since some of the high-harmonic cavities would be replaced by the lower-harmonic cavities.

### EFFECTIVE PILE-UP DENSITY

The pile-up (PU) density  $\rho(x, y, s, t)$  describes the distribution of events in space and time during the collision of two bunches. By projecting this density along longitudinal coordinate  $s$  (with the interaction point at  $s = 0$ ), integrating over the domain of the remaining coordinates, the line pile-up density  $\rho(s)$  is defined, and similar projections can be made for the other coordinates. The total pile up (or simply pile-up) is the number of events per bunch crossing and it is equal to  $\mu = \sigma \mathcal{L}/(n_b f)$  where  $\mathcal{L}$  is the luminosity,  $\sigma$  the inelastic cross section,  $n_b$  the number of colliding bunches and  $f$  their revolution frequency. These parameters evolve with time.

Let us denote the time in the fill as  $T$ ; we define the *effective line pile-up density* [2] as the average of the line PU density over the fill duration  $T_{\text{fill}}$  weighted by the total integrated pile-up. Formally,

$$\bar{\rho} \equiv \frac{\int_0^{T_{\text{fill}}} \mu(T) E[\rho(s; T)] dT}{\int_0^{T_{\text{fill}}} \mu(T) dT}, \quad (5)$$

where  $\mu(T)$  and  $\rho(s; T)$  are the total PU and line PU density at time  $T$ , respectively, and

$$E[\rho(s; T)] = \int_{-\infty}^{\infty} \rho(s; T) \frac{\rho(s; T)}{\mu(T)} ds, \quad (6)$$

is the expected value of  $\rho$  over  $s$  with probability  $\rho(s; T)/\mu(T)$ . The lower the effective line PU density is, the higher the detector efficiency becomes for the reconstruction of event vertices.

## RESULTS

The nominal and ultimate levelled luminosities yield a total pile-up of 132 and 197 events per bunch crossing, respectively, for all scenarios except in the 8b+4e case where

these values are set slightly higher. The effect of the levelling can be seen in Fig. 1. The fill duration and levelling times are listed in Table 2, which in the case of the current nominal baseline, correspond to 7.8 h and 5.8 h, and their ratio does not remain constant in the ultimate operation.

Simulations with the q-Gaussian bunch profile show a generalized increase of the integrated luminosity by 2% with respect to the Gaussian distribution for all the scenarios at the nominal operation; the ultimate performance, however, does not have a significant change with the new bunch profile. In the case of the HL-LHC nominal baseline, the integrated luminosity is  $234 \text{ fb}^{-1}$  per year (160 days), and it is reduced by 24%, 2%, 10% for the 8b+4e, 200 MHz and No CC scenarios, respectively; the performance is retained in the Flat case. The ultimate integrated luminosity corresponds to an increment of nearly 40% with respect to the nominal.

A detailed characterization of the RMS luminous region and RMS luminous time at the beginning and at the end of the levelling process is listed in Table 3. The results show that the use of the q-Gaussian description of the bunch profile leads to a reduction of the RMS luminous region from 51 mm to 48 mm for the nominal baseline at the start of the fill when compared to previous studies with Gaussian. The RMS luminous region reduces by 10% to 20% at the end of fill, except of the Flat option, where it only reduces by 5%. The largest luminous region ( $\sim 80 \text{ mm}$ ) is delivered by 200 MHz. For all scenarios, the RMS luminous time remains almost

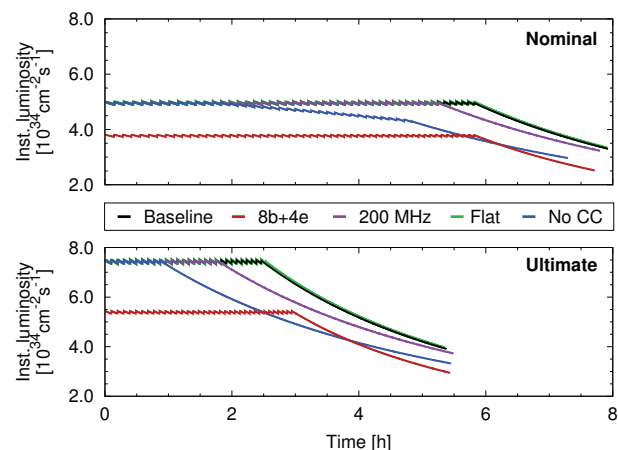


Figure 1: Instantaneous luminosity for the HL-LHC baseline and alternative scenarios.

Table 3: RMS Luminous Region and Time, and Effective PU Densities for the HL-LHC Baseline and Alternative Scenarios

| Parameter                 | Unit             | Nominal  |       |         |      |       | Ultimate |       |         |      |       |
|---------------------------|------------------|----------|-------|---------|------|-------|----------|-------|---------|------|-------|
|                           |                  | Baseline | 8b+4e | 200 MHz | Flat | No CC | Baseline | 8b+4e | 200 MHz | Flat | No CC |
| <i>Start of levelling</i> |                  |          |       |         |      |       |          |       |         |      |       |
| RMS luminous region       | mm               | 48.2     | 49.5  | 79.0    | 53.0 | 42.7  | 45.8     | 47.8  | 74.3    | 52.3 | 37.6  |
| RMS luminous time         | ps               | 179      | 179   | 289     | 179  | 186   | 179      | 179   | 286     | 179  | 188   |
| Peak line PU density      | mm <sup>-1</sup> | 1.05     | 1.09  | 0.64    | 0.95 | 1.22  | 1.67     | 1.61  | 1.03    | 1.45 | 2.09  |
| Peak time PU density      | ps <sup>-1</sup> | 0.28     | 0.30  | 0.18    | 0.28 | 0.27  | 0.42     | 0.43  | 0.27    | 0.42 | 0.39  |
| <i>End of levelling</i>   |                  |          |       |         |      |       |          |       |         |      |       |
| RMS luminous region       | mm               | 41.5     | 43.5  | 66.0    | 50.4 | 35.3  | 41.5     | 43.2  | 67.9    | 50.4 | 35.2  |
| RMS luminous time         | ps               | 179      | 178   | 260     | 180  | 189   | 179      | 178   | 275     | 180  | 190   |
| Peak line PU density      | mm <sup>-1</sup> | 1.26     | 1.27  | 0.79    | 1.01 | 1.30  | 1.88     | 1.83  | 1.16    | 1.52 | 2.24  |
| Peak time PU density      | ps <sup>-1</sup> | 0.28     | 0.30  | 0.20    | 0.28 | 0.23  | 0.43     | 0.43  | 0.28    | 0.42 | 0.39  |
| Effective line PU density | mm <sup>-1</sup> | 0.79     | 0.81  | 0.49    | 0.68 | 0.87  | 1.14     | 1.13  | 0.67    | 0.95 | 1.21  |
| Effective time PU density | ps <sup>-1</sup> | 0.20     | 0.21  | 0.13    | 0.20 | 0.17  | 0.27     | 0.28  | 0.17    | 0.27 | 0.22  |

constant along the entire fill, with a magnitude between 180 ps and 190 ps for any scenario (except for 200 MHz, with 260 ps and 290 ps due to longer bunch length).

A limit of 1.30 events/mm on the maximum peak pile-up density along the fill is imposed in the simulation at nominal levelling to the alternative without CCs. The maximum peak values take place at the end of the levelling and, in the case of the baseline HL-LHC, its magnitude is 1.26 events/mm. A maximum peak value of  $\sim 2.2$  events/mm is reached in the absence of CCs in the ultimate operation. In Fig. 2 the line PU densities for each scenario at the beginning of the fill are displayed, together with their corresponding Gaussian fits. The Gaussian description of the line PU densities, as well as the time PU densities, prove to be satisfactory, and their parameters (RMS and peak) are close to those in Table 3.

The effective line PU density, computed from Eq. (5), is 0.79 events/mm for the nominal baseline (compare to 0.76 events/mm for the case with Gaussian profile). The 200 MHz has a remarkably low value of  $\sim 0.5$  events/mm. The largest values are delivered by the 8b+4e scenario and

in the absence of CCs, while the Flat optics improves this parameter by reducing its magnitude slightly. In the ultimate operation,  $\bar{\rho}$  increases by around 40 % for all cases and, in particular, its value is 1.14 events/mm for the baseline.

## CONCLUSION

Studies with the latest description of the longitudinal bunch profile make use of the q-Gaussian distribution. The simulations show an increment of 2 % on the integrated luminosity and a reduction of the RMS luminous region by 5 % for the nominal baseline. The effective line pile-up density, a new figure-of-merit that allows the comparison of the performance of the different scenarios and that takes into account the evolution of the PU and line PU density, reaches around 0.8 events/mm for the a baseline HL-LHC.

The adoption of a  $12.5\sigma$ -beam separation has little to negligible impact in the scenarios with flat optics. The Flat option achieves the baseline integrated luminosity and reduces the effective line PU density. In the same way, the use of flat optics with 200 MHz has made of it a very attractive operational alternative in the case of e-cloud limitations due to its low reduction of integrated luminosity and very low effective line PU density; nevertheless, this case delivers the largest RMS luminous region, requiring an evaluation of the detector performance loss. The scenario without CCs not only exhibits a lower integrated luminosity, but a higher effective line PU density.

These results are used in the comparison of the various scenarios taking into account the dependence of the detector event reconstruction efficiency which depends on the pile-up and pile-up density.

## ACKNOWLEDGEMENT

The authors thank the Experimental Data Quality group for fruitful discussions that led to the introduction of the concept of effective pile-up density, to Y. Papaphilippou for comments on the q-Gaussian distribution, and to M. Giovannozzi for his comments on this paper.

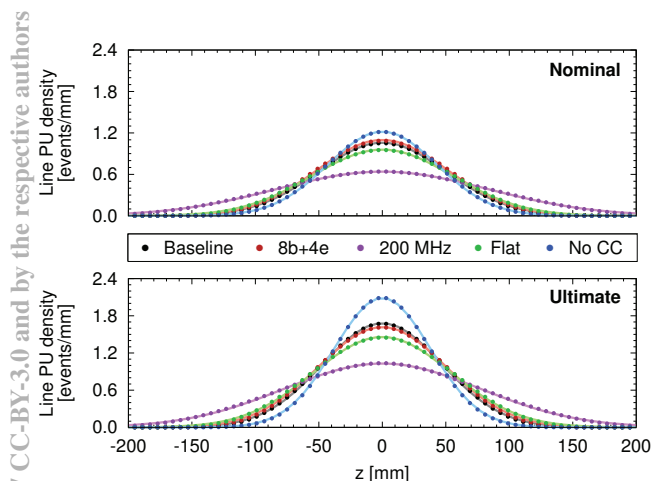


Figure 2: Line PU density (dotted line) and Gaussian fit (solid line) at the start of the fill for the HL-LHC baseline and alternative scenarios.

## REFERENCES

- [1] “High-luminosity Large Hadron Collider (HL-LHC) Technical Design Report V0”, edited by G. Apollinari, I. Béjar Alonso, O. Brüning, M. Lamont, and L. Rossi, pp. 49–56; Geneva, 2015, unpublished. <https://edms.cern.ch/ui/doc/1558149>
- [2] R. Tomás, “Updated optics layout and machine performance”, 6th HL-LHC Collaboration Meeting, Paris, Nov., 2016. <https://indico.cern.ch/event/549979/contributions/2257122/attachments/1370681/2079634/SLIDESBeamer.pdf>
- [3] E. Shaposhnikova and J.E. Muller, “Longitudinal stability limits and bunch length specifications”, 78th HL-LHC WP2 Meeting, Sep. 2016. [https://indico.cern.ch/event/563288/contributions/2308739/attachments/1342048/2021482/HLLHC\\_WP2\\_v1.pdf](https://indico.cern.ch/event/563288/contributions/2308739/attachments/1342048/2021482/HLLHC_WP2_v1.pdf)
- [4] L. Medina, “Update on beam parameters and operation schemes”, Ninth Experimental Data Quality Meeting, Apr. 2016. [https://indico.cern.ch/event/626264/contributions/2529217/attachments/1442351/2221162/2017-04-10\\_HLLHC-EDQ.pdf](https://indico.cern.ch/event/626264/contributions/2529217/attachments/1442351/2221162/2017-04-10_HLLHC-EDQ.pdf)
- [5] D. Pellegrini, S. Fartoukh, N. Karastathis, and Y. Papaphilipou, “Multiparametric response of the HL-LHC dynamic aperture in presence of beam-beam effects”, presented at the 8th International Particle Accelerator Conference (IPAC’17), Copenhagen, Denmark, May 2017, paper TUPVA010, this conference.
- [6] E. Shaposhnikova and J.E. Muller, “Bunch length and particle distribution for (HL-)LHC”, 82nd HL-LHC WP2 Meeting, Jan. 2017. [https://indico.cern.ch/event/572439/contributions/2423329/attachments/1394442/2125205/HL-LHC\\_WP2\\_Jan17.pdf](https://indico.cern.ch/event/572439/contributions/2423329/attachments/1394442/2125205/HL-LHC_WP2_Jan17.pdf)
- [7] S. Papadopoulou *et. al.*, “Modelling and measurements of bunch profiles at the LHC”, presented at the 8th International Particle Accelerator Conference (IPAC’17), Copenhagen, Denmark, May 2017, paper TUPVA044, this conference.
- [8] B. Petersen, “ATLAS upgrade status and outlook”, ECFA High Luminosity LHC Experiments Workshop 2016, Oct. 2016, <https://indico.cern.ch/event/524795/contributions/2235126/attachments/1346960/2031430/StatusAndPlans.pdf>
- [9] P. Azzi, “CMS performance: Dependence on scenario for luminous region”, ECFA High Luminosity LHC Experiments Workshop 2016, Oct. 2016, [https://indico.cern.ch/event/524795/contributions/2235253/attachments/1347082/2031647/EDQCMS\\_ECFA\\_Azzi.pdf](https://indico.cern.ch/event/524795/contributions/2235253/attachments/1347082/2031647/EDQCMS_ECFA_Azzi.pdf)
- [10] S. Umarov, C. Tsallis, and S. Steinberg, “On a q-central limit theorem consistent with nonextensive statistical mechanics”, *Milan Journal of Mathematics*, vol. 76, no. 1, pp. 307–328, 2008, <http://dx.doi.org/10.1007/s00032-008-0087-y>, doi:10.1007/s00032-008-0087-y
- [11] L. Medina and R. Tomás, “Performance and operational aspects of HL-LHC scenarios”, in *Proc. 7th International Particle Accelerator Conference (IPAC’16)*, Busan, Korea, May 2016, paper TUPMW035, pp. 1516–1519, ISBN: 978-3-95450-147-2, <http://jacow.org/ipac2016/papers/tupmw035.pdf>, doi:10.18429/JACoW-IPAC2016-TUPMW035, 2016.
- [12] E. Shaposhnikova and J.E. Müller, “Possible beam parameters in double RF operation of the CERN LHC”, in *Proc. 7th International Particle Accelerator Conference (IPAC’16)*, Busan, Korea, Mar. 2016, paper WEPMW008, pp. 2430–2433, ISBN: 978-3-95450-147-2, <http://jacow.org/ipac2016/papers/wepmw008.pdf>, doi:10.18429/JACoW-IPAC2016-WEPMW008, 2016.